4090–4095 *Nucleic Acids Research, 2005, Vol. 33, No. 13*
doi:10.1093/nar/gki721

Topological constraints in nucleic acid hybridization kinetics

Justin S. Bois, Suvir Venkataraman[1], Harry M. T. Choi[1], Andrew J. Spakowitz, Zhen-Gang Wang and Niles A. Pierce[1,2,*]

Department of Chemical Engineering, [1]Department of Bioengineering and [2]Department of Applied and Computational Mathematics, California Institute of Technology, Pasadena, CA 91125, USA

Received April 24, 2005; Revised May 17, 2005; Accepted July 4, 2005

ABSTRACT

A theoretical examination of kinetic mechanisms for forming knots and links in nucleic acid structures suggests that molecules involving base pairs between loops are likely to become topologically trapped in persistent frustrated states through the mechanism of 'helix-driven wrapping'. Augmentation of the state space to include both secondary structure and topology in describing the free energy landscape illustrates the potential for topological effects to influence the kinetics and function of nucleic acid strands. An experimental study of metastable complementary 'kissing hairpins' demonstrates that the topological constraint of zero linking number between the loops effectively prevents conversion to the minimum free energy helical state. Introduction of short catalyst strands that break the topological constraint causes rapid conversion to full duplex.

INTRODUCTION

In studies of nucleic acid thermodynamics (1–4) and kinetics (5,6), the molecular state space is often described in terms of secondary structure (i.e. the list of base pairs). This useful simplification neglects topological effects that arise from the fact that strands cannot pass through each other. Intertwining of strands is a common occurrence in nucleic acid structures, as stacking interactions between adjacent base pairs ensure that the strands wrap around each other in a helical fashion. This phenomenon has been exploited by Seeman and co-workers (7) to design structures with knotted and linked topologies that employ both the right-handed helicity of B-DNA and the left-handed helicity of Z-DNA.

Nucleic acid strand topology plays an important role in biological processes as well. DNA replication and recombination involve enzyme-mediated formation and resolution of double-stranded knots and catenanes (8). Topological effects also influence the regulatory mechanisms of antisense RNAs that undergo loop–loop interactions with target mRNAs to inhibit transcription or translation (9). The resulting metastable 'kissing' complexes formed by rapid base pairing between complementary loops relax sufficiently slowly to the full duplex state that the stable duplex is believed to be biologically irrelevant (9). It is precisely this slow relaxation to equilibrium that makes kissing loop complexes attractive candidates for storing potential energy for DNA nanotechnology applications. In principle, autonomous DNA machines can be powered by using catalyst strands to accelerate this relaxation process (10).

Here, we examine the theoretical consequences of topology on the hybridization kinetics of RNA and single-stranded DNA (ssDNA) molecules and elucidate the nature of the topological constraints that govern the metastability of kissing complementary loops. This topological viewpoint suggests that hybridization catalysts (10,11) can facilitate rapid relaxation to the stable duplex state by breaking a topological constraint. Experimental analysis of a metastable kissing hairpin system and a corresponding hybridization catalyst suggests that manipulation of strand topology is an effective means of engineering conditional metastability.

METHODS

System specifications

The DNA sequences for the two hairpin strands (H1 and H2) and the catalyst strand (C) are defined in Figure 2. For the kinetic studies, H1 is replaced by H1L, which is labeled on the 5′ end with TET (Applied Biosystems) and on the 3′ end with BHQ1 (Biosearch Technologies). DNA oligos were

*To whom correspondence should be addressed at Caltech, Mail Code 114-96, Pasadena, CA 91125, USA. Tel: +1 626 395 8086; Fax: +1 626 395 8845; Email: niles@caltech.edu

The authors wish it to be known that, in their opinion, the first two authors should be regarded as joint First Authors

synthesized, labeled and purified (PAGE for H1, H2 and C; dual HPLC for H1L) by Integrated DNA Technologies. Stock solutions were prepared in ultrapure H_2O (Barnstead Nanopure) and concentrations were determined at 260 nm using molecular extinction coefficients provided by the supplier.

Sequence design

Different subsets of the two hairpin sequences were designed so as to simultaneously optimize affinity and specificity (12) for four target structures: (i) sequence H1 forming a hairpin structure with a 10 bp stem and a 20 base loop, (ii) sequence H2 forming the same hairpin structure, (iii) the 20 base loop sequences of H1 and H2 forming a 20 bp helix (to optimize kissing) and (iv) the full H1 and H2 sequences forming a 40 bp helix (to optimize the full duplex). This was accomplished by maximizing an objective function corresponding to the product of four probabilities $p(\mathrm{H1})\cdot p(\mathrm{H2})\cdot p(\mathrm{loop})\cdot p(\mathrm{full})$ subject to the constraint of sequence symmetry minimization (13) with a word length of four. The probabilities were calculated using loop-based nearest-neighbor free energy parameters for ssDNA at 37°C (3) and a dynamic programming partition function algorithm that accounts for all unpseudoknotted secondary structures (14). Since this algorithm applies to single strands, design targets with two strands were modeled using an AAAA linker between the strands. Sequences were designed using an adaptive walk starting from a random initial sequence for H1 (H2 is the reverse complement and C is the reverse complement of the 3′ half of H2). At each step, a random base (in a loop) or base pair (in a stem) mutation was accepted if the objective function improved. The design selected for experimental study had the maximum objective function out of 1000 independent designs, each obtained via an adaptive walk that was terminated after 5000 consecutive mutations were rejected.

Native gel electrophoresis

Stock solutions of 20 μM H1, H2 and C strands were prepared using ultrapure H_2O. Aliquots of stock solutions were heated to 90°C for 90 s, quenched on ice for 40 s and then allowed to equilibrate to room temperature for 30 min on the bench top. Reactions were run overnight at room temperature in TAE/Mg^{2+} buffer (40 mM Tris, 19 mM acetic acid, 1 mM EDTA and 12.5 mM magnesium acetate, pH 8.0). For each lane, the reaction was performed by combining 0.75 μl of each relevant oligo with 1.5 μl of 10× TAE/Mg^{2+} buffer, diluting to a 12 μl reaction volume (1.25 μM oligo reaction concentration), and mixing by pipetting. For annealed lanes, samples were heated to 90°C for 3 min and then slow-cooled to room temperature by turning off the heat block and leaving the samples on the heat block for 3 h. Before loading the samples on a gel, reacted samples were supplemented with 3 μl of sample loading buffer: 50 mM Tris–HCl (pH 8.0), 25% glycerol, 5 mM EDTA, 0.2% bromophenol blue, 0.2% xylene cyanole FF (Bio-Rad). Samples were run in an 18% polyacrylamide gel with 1× TAE/Mg^{2+} buffer at 120 V for 4 h. The buffer temperature was controlled to maintain the samples at 8°C throughout the run. The gel was stained with Sybr Gold (Molecular Probes), excited at 495 nm and imaged with a 530 nm bandpass filter on a Bio-Rad Molecular Imager FX gel scanner.

Kissing hairpin complex purification

Overnight reactions were performed on six identical samples containing 5 μl of 20 μM stock of each hairpin, 0.5 μl ultrapure H_2O and 1.5 μl of 10× TAE/Mg^{2+} buffer (12 μl reaction volume and 8.33 μM reaction concentration). After annealing one sample as above (to identify the full duplex state), native gel electrophoresis was then performed on six lanes using the same protocol as above. The kissing hairpin bands were cut out of the five unannealed lanes and the DNA complex was electroeluted (Schleicher and Schuell Elutrap). The eluted complex was then quantified by annealing a fraction of the sample and comparing the absorbance at 260 nm to that of annealed duplex formed from previously quantified hairpins. For the fluorescence kinetics experiments, the fluorescent-labeled H1L was used in place of H1. For these reaction conditions, the labeled kissing hairpin band was visible without staining.

Fluorescence kinetics

Fluorescence data were obtained using a fluorometer from Photon Technology International with the temperature controller set to 23°C. Excitation and emission wavelengths were 521 and 541 nm, respectively, with 4 nm bandwidths. Stock solutions of 2.4 μM purified H1L/H2 complex and 10 μM C were prepared in TAE/Mg^{2+} buffer. Reactions were performed by adding 25 μl of the H1L/H2 complex to 2969 μl of reaction buffer and mixing by gentle pipetting for ≈30 s. The run was paused after 60 min for ≈30 s to add 6 μl of C at the required concentration and mix by gentle pipetting (10 μM C for 1× corresponding to 20 nM concentrations for all species, 5 μM C for 0.5×, 2.5 μM C for 0.25×, 1 μM C for 0.1×, 0.1 μM for 0.01× and reaction buffer for the control). After 180 min of data acquisition, the samples were annealed as for gel electrophoresis, and then data acquisition was resumed for 60 min.

KNOTTING AND LINKING MECHANISMS

We begin with a brief theoretical examination of alternative kinetic mechanisms by which topological features can arise in nucleic acid structures. A strand of RNA or ssDNA that bends back on itself to form a helix creates a loop of unpaired bases that can participate in the formation of knots or links. The simplest non-trivial topological scenario for a nucleic acid strand is the self-knotting of a hairpin loop (Figure 1a). A traditional hairpin secondary structure representation would contain only base pairing information and omit this topological detail. In considering the behavior of such a molecule, is it justifiable to assume that the loop is unknotted?

Comparison of measured loop closure times for ssDNA hairpins (15) with simulated first contact times for the ends of a Rouse chain (a phantom chain of beads on springs) (16) reveals that the loop closure time is typically orders of magnitude longer than the first contact time of the ends. (See the Appendix for details.) Hence, the probability of chain entanglement at equilibrium can be used to estimate the likelihood of becoming kinetically trapped in knotted hairpin conformations. The probability of knotting grows slowly from zero to

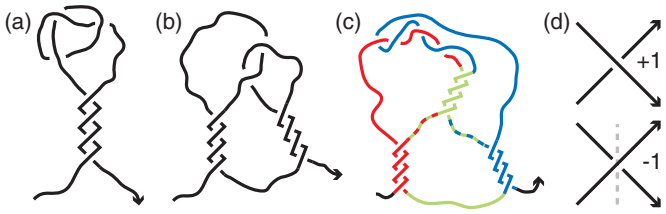

Figure 1. (**a**) A knotted hairpin loop. (**b**) Linked hairpin loops. (**c**) Kissing hairpin loops. (**d**) The sign convention for crossings in a projected structure. Positive and negative signs correspond to left-handed and right-handed wrapping of antiparallel strands, respectively. For clarity, the dashed line in the −1 crossing corresponds to the longitudinal axis of a right-handed helix. Arrowheads denote the 3′ end of each strand.

unity as the chain length increases; a freely jointed chain with a loop of ≈250 bases has roughly a 25% chance of being knotted (17,18) [Based on a statistical length (twice the persistence length) of ≈2.5 bases for ssDNA (19)]. Hence, the probability of self-knotting in short nucleic acid loops is small (20) and the practice of assuming that hairpin secondary structures contain no knots is often justified.

A similar argument applies to the formation of linked hairpins (that do not base pair in the looped regions) as depicted in Figure 1b. The disparity in time scales between diffusive conformational sampling and helix nucleation suggests that entanglements should become kinetically trapped to form links between loops with roughly the probability that these states are expected to exist in the equilibrium ensemble. Again, the probability of entanglement is low for chains that are not too long and grows slowly to unity as the chain length increases (17,18).

In contrast to the previous cases, structures featuring interloop base pairing are more likely to have entanglements between the single-stranded sections of the loops due to a process we term 'helix-driven wrapping'. This mechanism is illustrated by the kissing hairpins of Figure 1c. Consider the folding pathway in which the red and blue helices nucleate before the green helix. In that case, formation of the green helix causes the green regions to wrap around each other in a right-handed fashion, causing the adjacent single-stranded regions to wrap in a left-handed fashion. (For simplicity, we assume that all helices are right-handed B-DNA and that left-handed wrappings remain single-stranded.) This left-handed wrapping is topologically trapped in the sense that it cannot be alleviated without breaking a helix. This phenomenon occurs whenever two loops hybridize to each other; every full turn of a helix must be accompanied by a left-handed wrap.

There are other folding pathways that could trap left-handed wrapping. If the red helix forms first, the left-handed wrapping incurred by subsequent formation of the green helix is not immediately trapped because the blue loop is not yet closed. Although the left-handed wrapping is helix-driven and not a consequence of random diffusion through conformational space, a diffusive unthreading process is required to eliminate it. If this process is slower than the nucleation of the blue helix (as would be the case if the loops were small and the wrapped chain must undergo a sterically hindered unthreading through the loop), the blue helix can form while none, some, or all of the left-handed wrapping is still present.

FREE ENERGY LANDSCAPE CONSEQUENCES

The effects of topological constraints on folding kinetics can be considered in the context of the free energy landscape, an important conceptual tool in describing heteropolymer folding (21,22). Each point on the landscape is the free energy of a state of the system. In a departure from traditional treatments, we include topological information in addition to the secondary structure in defining each state.

The topology of loop–loop interactions in nucleic acid structures can be characterized by the linking number (Lk), defined as half the sum of all the signed crossings in a projection of the structure onto a plane (following the sign convention of Figure 1d) (23). For the kissing hairpins of Figure 1c, the negative crossings of the right-handed green helix and the positive crossings of the left-handed wrapping between the red and the blue strands cancel out, giving $Lk = 0$ for the red and blue loops. The left-handed wrapping can be redistributed to the dashed regions by twisting the green helix around its longitudinal axis, but the topological constraint of zero linking number cannot be alleviated without breaking the secondary structure. Although the linking number does not provide sufficient information to distinguish all possible links (23), its simplicity makes it attractive for characterizing DNA hybridization topologies. More complicated classification methods (23–25) can be adopted if knots and larger classes of links must be described for particular hybridization pathways of interest.

Two states on the free energy landscape are close to each other if the molecular rearrangement required to move from one to the other is small. For example, two hairpin loops with the same linking number that differ by a single base pair are very close on the landscape. The time scale required for the breakage (or formation) of the base pair is fast, since the states are separated by only a small barrier.

By contrast, two states may have exactly the same base pairs but different topologies and therefore can lie very far from each other on the landscape. For example, if the kissing hairpins in Figure 1c were to access an $Lk = -2$ state, either the red or blue helix would have to completely unpair, the resulting free end would have to diffuse through the remaining loop twice, and then the broken helix would have to reform. This constitutes a major rearrangement and occurs over a long time scale. Topological constraints can also influence the free energy of a state because of the restricted conformational space available to the molecule (18); two states differing only in topology can therefore lie at different energy levels on the landscape.

METASTABILITY VIA TOPOLOGY

Topological constraints can be exploited in designing molecules that become trapped in metastable structures far from the global minimum on the free energy landscape. The transition to equilibrium can be dramatically accelerated by introducing hybridization catalyst strands (10,11) that break the topological constraint.

Consider two complementary DNA hairpins (H1 and H2 of Figures 2 and 3) with 10 bp stems and 20 base loops that interact to form a 40 bp helix in their minimum free energy state. Stoichiometric mixing of H1 and H2 causes most of the

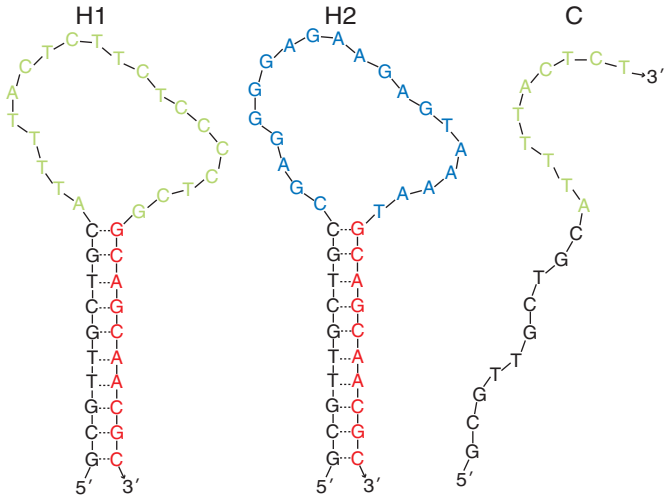

Figure 2. Sequences for complementary hairpins H1 and H2 and hybridization catalyst C.

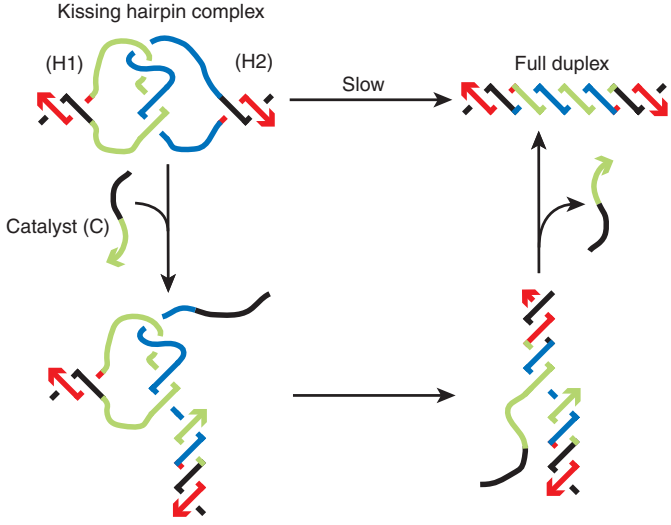

Figure 3. Putative topological effects in the conversion of kissing hairpins (H1 and H2) to the full duplex state. Base pairing between the complementary loops results in a metastable kissing hairpin complex that proceeds to the minimum free energy helical structure very slowly except in the presence of a catalyst strand (C) that opens H2 to break the topological constraint. Color use is consistent with the sequence definitions in Figure 2.

hairpins to hybridize in the complementary loops to form metastable kissing hairpin complexes (Figure 4). Gel electrophoresis suggests that conversion to the full duplex can be achieved either by annealing or by introducing a short DNA catalyst strand (C) that is complementary to the 3′ half of H2. The conversion rate between the metastable kissing hairpin complex and the full duplex can be examined using fluorescence quenching measurements (Figure 5). The topological constraint causes the kissing complex and full duplex to be sufficiently far apart on the free energy landscape that no conversion is observable on this experimental time scale. Stoichiometric introduction of catalyst strands causes rapid conversion to the full duplex. Catalytic turnover is confirmed by additional studies with substoichiometric catalyst concentrations.

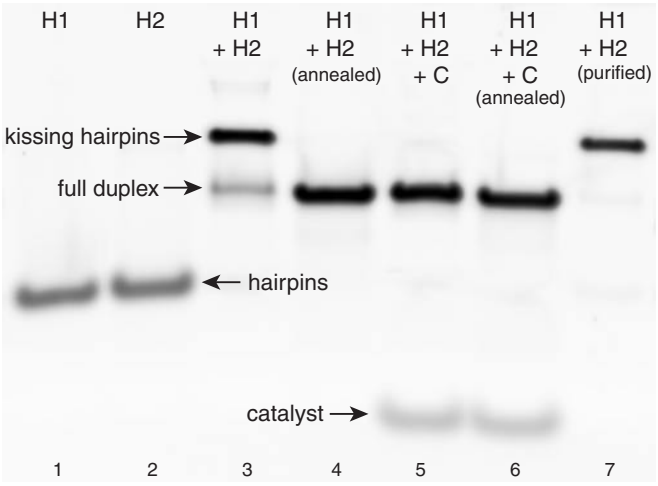

Figure 4. Native PAGE of the kissing hairpin system after overnight reactions. Lanes 1 and 2: H1 and H2 hairpins. Lane 3: the metastable kissing hairpin complex dominates the stable full duplex state. Lanes 4–6: conversion to full duplex is achieved by annealing (Lane 4) or by introducing a hybridization catalyst (lanes 5 and 6). Lane 7: purified kissing hairpin complex.

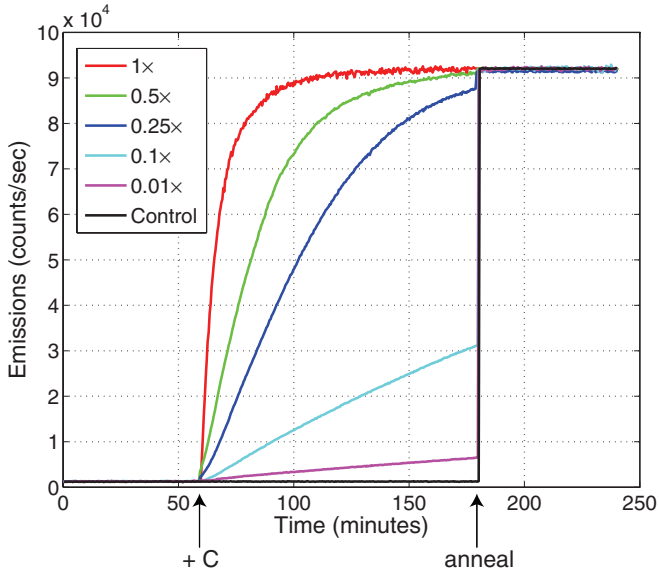

Figure 5. Fluorescence kinetics monitoring conversion of purified kissing hairpins to the full duplex state. No conversion is discernible in the absence of the hybridization catalyst (control). Rapid conversion to full duplex is observed upon introducing equimolar hybridization catalyst (1×). Substoichiometric catalyst concentrations demonstrate turnover, with the conversion rate decreasing monotonically with catalyst concentration. The hairpin H1 is labeled with a fluorophore on one end and a quencher on the other so that the bulk fluorescence increases as the conversion to the helical state proceeds. The samples are annealed to determine the equilibrium signal.

These kinetic trajectories are consistent with topologically induced metastability resulting from helix-driven wrapping between the complementary loops. Although the minimum free energy state is topologically trivial (there are no loops), formation of the inter-loop helix ensures that the folding pathway to achieve equilibrium is topologically constrained until one of the three helices is completely broken. The topological requirement that $Lk = 0$ between the loops implies severe steric hindrance to the conversion process. The catalyst strand

removes the topological constraint by opening the stem of H2 via a strand displacement branch migration. Additional topologically unhindered strand displacement interactions complete the conversion to the helical conformation and release the catalyst strand. Although the secondary structures are different, the identical topological argument can be used to explain the results of Seelig *et al*. (11), in which metastable complexes of DNA bulge loops are rapidly relaxed to minimum free energy helical conformations using hybridization catalysts that break the topological constraints via strand displacement interactions initiated at single-stranded extensions of the bulge loop helices.

In nature, antisense RNA/mRNA loop–loop interactions are used to regulate transcription and translation (9). Loop motifs increase the rate of complex formation between the antisense RNA and its target via kissing interactions, which subsequently proceed to more stable inhibitory complexes along topologically accessible folding pathways (9). In the well-studied case of the antisense RNA CopA, which provides translational control by binding to its mRNA target CopT, initial kissing between hairpin loops is followed by the formation of two short inter-loop helices and an additional inter-strand helix that stabilizes the complex and provides irreversible translational inhibition (26,27). Topologically, the scenario is identical to the kissing hairpins examined above—conversion to the full duplex is very slow *in vitro* and the minimum free energy helical conformation is thought to be biologically irrelevant (27–29).

Experimental evidence suggests that similar inhibitory mechanisms based on topologically trapped metastable complexes are also employed by other antisense RNA/mRNA pairs (9,30). Structural hypotheses about these metastable complexes can be guided by the topological requirement that $Lk = 0$ between complementary kissing loops, eliminating from consideration those secondary structures that are topologically infeasible (30,31).

In vivo, it is possible that RNA chaperone proteins (32) may assist RNA kissing complexes in folding to the full duplex state (9,33). Given the simplicity and effectiveness of nucleic acid hybridization catalysts in breaking topological constraints between complementary kissing loops, we speculate that nature may sometimes employ chaperone RNAs to assist in relaxing topological constraints that arise in RNA regulatory processes.

CONCLUSIONS

As nucleic acids fold, single loops may form knots and multiple loops may form links. In many cases, these topological effects are negligible, but for structures involving base pairing between loops, the mechanism of helix-driven wrapping increases the likelihood of adopting persistent frustrated states with entanglement between single-stranded regions. For this mechanism, the formation of a right-handed helix induces left-handed wrapping of the single-stranded regions at either end of the helix. When one or more of these single-stranded regions is part of a small closed loop, the left-handed wrapping unthreads slowly, or in the case of helix formation between two existing loops, not at all. Trapping of left-handed wrapping creates a topological constraint that cannot be removed without breaking the secondary structure.

Inclusion of topology in the description of the molecular state space highlights the possibility that two molecules with the same secondary structure may be very far apart on the free energy landscape. As a result, topology can dramatically affect the kinetics and function of nucleic acid strands. In designing new hybridization reaction pathways, it is important to consider whether topological information adds critical features to a conceptual free energy landscape based solely on secondary structure.

Experimental studies of the kissing hairpin system suggest that the topological constraint of zero linking number can be used to engineer long-lived metastable complexes, and that the transition to equilibrium can be effectively catalyzed by introducing strands that break the constraint. The same topological constraint underlies the formation of metastable inhibitory complexes in the regulation of transcription and translation by antisense RNAs that recognize their target mRNAs by loop–loop kissing interactions. It is possible that nature has already discovered the idea of breaking topological constraints using chaperone RNAs.

ACKNOWLEDGEMENTS

We are grateful to J. Bloom for performing the initial experimental studies on the kissing hairpin system, to G.Seelig for discussions on hybridization catalysts, and to H. Isambert for discussions on the disparity in chain diffusion and helix nucleation time scales. This work was supported by the Charles Lee Powell Foundation (N.A.P.), the Ralph M. Parsons Foundation (N.A.P.), the NSF CAREER program (N.A.P.) and the Caltech Center for Biological Circuit Design (S.V.). Funding to pay the Open Access publication charges for this article was provided by NSF grant CCF-0448835.

Conflict of interest statement. None declared.

REFERENCES

1. de Gennes,P.-G. (1968) Statistics of branching and hairpin helices for the dAT polymer. *Biopolymers*, **6**, 715–729.
2. Chen,S.-J. and Dill,K.A. (1995) Statistical thermodynamics of double-stranded polymer molecules. *J. Chem. Phys.*, **103**, 5802–5813.
3. SantaLucia,J.,Jr (1998) A unified view of polymer, dumbbell, and oligonucleotide DNA nearest-neighbor thermodynamics. *Proc. Natl Acad. Sci. USA*, **95**, 1460–1465.
4. Mathews,D.H., Sabina,J., Zuker,M. and Turner,D.H. (1999) Expanded sequence dependence of thermodynamic parameters improves prediction of RNA secondary structure. *J. Mol. Biol.*, **288**, 911–940.
5. Flamm,C., Fontana,W., Hofacker,I.L. and Schuster,P. (2000) RNA folding at elementary step resolution. *RNA*, **6**, 325–338.
6. Isambert,H. and Siggia,E.D. (2000) Modeling RNA folding paths with pseudoknots: application to hepatitis delta virus ribozyme. *Proc. Natl Acad. Sci. USA*, **97**, 6515–6520.
7. Seeman,N.C. (1998) Nucleic acid nanostructures and topology. *Angew. Chem. Int. Ed.*, **37**, 3220–3238.
8. Wasserman,S.A. and Cozzarelli,N.R. (1986) Biochemical topology: applications to DNA recombination and replication. *Science*, **232**, 951–960.
9. Brunel,C., Marquet,R., Romby,P. and Ehresmann,C. (2002) RNA loop–loop interactions as dynamic functional motifs. *Biochimie*, **84**, 925–944.
10. Turberfield,A.J., Mitchell,J.C., Yurke,B., Mills,A.P.,Jr, Blakey,M.I. and Simmel,F.C. (2003) DNA fuel for free-running nanomachines. *Phys. Rev. Lett.*, **90**, 118102.

11. Seelig,G., Yurke,B. and Winfree,E. (2005) DNA hybridization catalysts and catalyst circuits. In *DNA Computing: 10th International Meeting on DNA Based Computers*. Lecture Notes in Computer Science, Springer, In press.
12. Dirks,R.M., Lin,M., Winfree,E. and Pierce,N.A. (2004) Paradigms for computational nucleic acid design. *Nucleic Acids Res.*, **32**, 1392–1403.
13. Seeman,N.C. (1982) Nucleic acid junctions and lattices. *J. Theor. Biol.*, **99**, 237–247.
14. McCaskill,J.S. (1990) The equilibrium partition function and base pair binding probabilities for RNA secondary structure. *Biopolymers*, **29**, 1105–1119.
15. Goddard,N.L., Bonnet,G., Krichevsky,O. and Libchaber,A. (2000) Sequence dependent rigidity of single stranded DNA. *Phys. Rev. Lett.*, **85**, 2400–2403.
16. Pastor,R.W., Zwanzig,R. and Szabo,A. (1996) Diffusion limited first contact of the ends of a polymer: comparison of theory with simulation. *J. Chem. Phys.*, **105**, 3878–3882.
17. Grosberg,A.Y. and Kholkhlov,A.R. (1994) *Statistical Physics of Macromolecules*. American Institute of Physics Press, NY, pp. 75.
18. Kholodenko,A.L. and Vilgis,T.A. (1998) Some geometrical and topological problems in polymer physics. *Phys. Rep.*, **298**, 251–370.
19. Smith,S.B., Cui,Y.J. and Bustamante,C. (1996) The overstretching of B-DNA: the elastic response of individual double-stranded and single-stranded DNA molecules. *Science*, **271**, 795–799.
20. Wiegel,F.W. (1983) Conformational phase transitions in a macromolecule: exactly solvable models. In Domb,C. and Lebowitz,D.L. (eds), *Phase Transitions and Critical Phenomena*. Academic Press, London, Vol. 7, pp. 101–149.
21. Onuchic,J.N., Luthey-Schulten,Z. and Wolynes,P.G. (1997) Theory of protein folding: the energy landscape perspective. *Annu. Rev. Phys. Chem.*, **48**, 545–600.
22. Chen,S.-J. and Dill,K.A. (2000) RNA folding energy landscapes. *Proc. Natl Acad. Sci. USA*, **97**, 646–651.
23. Adams,C.C. (1994) *The Knot Book: An Elementary Introduction to the Mathematical Theory of Knots*. W.H. Freeman, NY.
24. White,J.H. and Cozzarelli,N.R. (1984) A simple toplogical method for describing stereoisomers of DNA catenanes and knots. *Proc. Natl Acad. Sci. USA*, **81**, 3322–3326.
25. White,J.H., Millett,K.C. and Cozzarelli,N.R. (1987) Description of the topological entanglement of DNA catenanes and knots by a powerful method involving strand passage and recombination. *J. Mol. Biol.*, **197**, 585–603.
26. Kolb,F.A., Malmgren,C., Westhof,E., Ehresmann,C., Ehresmann,B., Wagner,E.G.H. and Romby,P. (2000) An unusual structure formed by antisense-target RNA binding involves an extended kissing complex with a four-way junction and a side-by-side helical alignment. *RNA*, **6**, 311–324.
27. Kolb,F.A., Engdahl,H.M., Slagter-Jager,J.G., Ehresmann,B., Ehresmann,C., Westhof,E., Wagner,E.G.H. and Romby,P. (2000) Progression of a loop–loop complex to a four-way junction is crucial for the activity of a regulatory antisense RNA. *EMBO J.*, **19**, 5905–5915.
28. Malmgren,C., Wagner,E.G.H., Ehresmann,C., Ehresmann,B. and Romby,P. (1997) Antisense RNA control of plasmid R1 replication. *J. Biol. Chem.*, **272**, 12508–12512.
29. Wagner,E.G.H. and Brantl,S. (1998) Kissing and RNA stability in antisense control of plasmid replication. *Trends Biochem. Sci.*, **23**, 451–454.
30. Kolb,F.A., Westhof,E., Ehresmann,B., Ehresmann,C., Wagner,E.G.H. and Romby,P. (2001) Four-way junctions in antisense RNA–mRNA complexes involved in plasmid replication control: a common theme? *J. Mol. Biol.*, **309**, 605–614.
31. Asano,K. and Mizobuchi,K. (2000) Structural analysis of late intermediate complex formed between plasmid ColIb-P9 Inc RNA and its target RNA. *J. Biol. Chem.*, **275**, 1269–1274.
32. Herschlag,D. (1995) RNA chaperones and the RNA folding problem. *J. Biol. Chem.*, **270**, 20871–20874.
33. Zhang,W. and Chen,S.-J. (2002) RNA hairpin-folding kinetics. *Proc. Natl Acad. Sci. USA*, **99**, 1931–1936.

APPENDIX

Chain diffusion and helix nucleation time scales

Libchaber and co-workers (15) observed that the loop closure time for a DNA hairpin with a 30 base loop and a 5 bp stem was ≈30 μs for a poly(T) loop and ≈110 μs for a poly(A) loop at ≈37°C. Neglecting sequence-dependent stiffness, the statistical length (twice the persistence length) of ssDNA is taken to be $b \approx 1.5$ nm ≈ 2.5 bases (19), corresponding to 11.8 statistical lengths for a loop of 30 bases. For a Rouse chain of this length, the Brownian dynamics simulations of Pastor *et al.* (16) estimate the first passage time for the ends to diffuse to within one statistical length of each other as $\approx 6.3b^2/D$, where D is the diffusivity of a Rouse bead. For a Rouse bead with diameter b, the Stokes–Einstein relation gives $D = kT/(3\pi\eta b)$, where the viscosity of water is taken to be $\eta \approx 0.7$ cP. The resulting diffusive first passage time is ≈0.03 μs, suggesting that the ends diffuse near each other many times before nucleating to form a helix.